Theta Oscillations Modulate Attentional Search Performance Periodically

Laura Dugué[1,2], Philippe Marque[3], and Rufin VanRullen[1,2]

Abstract

■ Visual search—finding a target element among similar-looking distractors—is one of the prevailing experimental methods to study attention. Current theories of visual search postulate an early stage of feature extraction interacting with an attentional process that selects candidate targets for further analysis; in difficult search situations, this selection is iterated until the target is found. Although such theories predict an intrinsic periodicity in the neuronal substrates of attentional search, this prediction has not been extensively tested in human electrophysiology. Here, using EEG and TMS, we study attentional periodicities in visual search. EEG measurements indicated that successful and unsuccessful search trials were associated with different amounts of poststimulus oscillatory amplitude and phase-locking at ~6 Hz and opposite prestimulus oscillatory phase at ~6 Hz. A trial-by-trial comparison of pre- and poststimulus ~6 Hz EEG phases revealed that the functional interplay between prestimulus brain states, poststimulus oscillations, and successful search performance was mediated by a partial phase reset of ongoing oscillations. Independently, TMS applied over occipital cortex at various intervals after search onset demonstrated a periodic pattern of interference at ~6 Hz. The converging evidence from independent TMS and EEG measurements demonstrates that attentional search is modulated periodically by brain oscillations. This periodicity is naturally compatible with a sequential exploration by attention, although a parallel but rhythmically modulated attention spotlight cannot be entirely ruled out. ■

INTRODUCTION

Models of visual search typically assume a hierarchical framework, in which lower levels decompose the visual input into distinct retinotopic feature maps (color, orientation, etc.), while higher levels perform attentional selection (Rodriguez-Sanchez, Simine, & Tsotsos, 2007; Deco, Pollatos, & Zihl, 2002; Itti & Koch, 2001; Treisman, 1998; Palmer, Ames, & Lindsey, 1993; Treisman & Gelade, 1980). Anatomically, the former areas could correspond to early cortical visual areas that receive the first bottom–up wave of activation within ~100 msec after stimulus onset (Thorpe & Fabre-Thorpe, 2001; VanRullen & Thorpe, 2001; Nowak, Munk, Girard, & Bullier, 1995), whereas the latter could involve higher-level regions of the frontal or parietal cortex such as FEF or PPC (Deco et al., 2002; Itti & Koch, 2001; Treisman, 1998). These areas have been proposed to subserve the function of a "master location map" (Wolfe, Cave, & Franzel, 1989; Treisman & Gelade, 1980) or "saliency map" (Itti & Koch, 2001). This attentional system selects the position of candidate targets in the visual array (e.g., the most salient elements) and focuses attention onto these elements (e.g., by sending feedback signals to lower levels; Saalmann, Pigarev, & Vidyasagar, 2007) to facilitate their processing and eventually permit the recognition of the target (when present). During an easy (or "pop-out") search, the target, because of its high salience or distinctiveness, will systematically be among the first selected elements; in difficult search tasks, however, target and distractors are equally likely to be selected initially, and successive iterations of the selection process will often be required until the target is found. In other words, these models predict that attentional selection should take place iteratively during difficult visual search.

This study was designed to test the following prediction: that the iterative selection characteristic of difficult search rests on a rhythmic (or periodic) neural process. We first demonstrate that the phase of EEG oscillations around the theta frequency (~6 Hz), just before the search array is presented, determines whether search will be successful or not—suggesting that the prestimulus ~6 Hz oscillation could index the ongoing state of the attention system; second, we find that the ~6 Hz EEG oscillation has a more consistent poststimulus phase and a higher amplitude in trials where search succeeds—suggesting that poststimulus ~6 Hz oscillations reflect the efficiency of target selection. These EEG oscillatory correlates are not observed for an easy ("pop-out") search task. Third, using TMS, we independently demonstrate that early visual areas contribute to search performance in a periodic manner (~6 Hz). Altogether, these converging results corroborate the prediction of standard search models of

[1]Université de Toulouse, [2]CNRS-CerCo, UMR 5549, Toulouse, France, [3]Médecine Physique et de Réadaptation, Toulouse, France

Journal of Cognitive Neuroscience 27:5, pp. 945–958
doi:10.1162/jocn_a_00755

an iterative selection during attentional search and point to the theta-band (4–8 Hz) of the EEG as a marker of this attentional periodicity.

METHODS

Participants

Twenty-nine participants (10 women), aged 20–36 years old, were recruited to participate in the difficult search experiment. Seven were excluded before performing the experiment because of their inability to perceive any TMS-induced phosphene with their eyes open (25% of the recruited participants; expected proportion based on the literature [e.g., Romei et al., 2008; Kammer, Puls, Erb, & Grodd, 2005]); another 10 were excluded because of the small size of their phosphenes, which would have precluded the presentation of search arrays within the corresponding area (see TMS Procedure). The 12 remaining participants performed the experiment. Two of them were excluded at the analysis stage because their search performance was at chance level in all conditions, including the no-TMS trials (control condition—see TMS Procedure). Finally, one participant's EEG data were excluded because too few trials remained after EEG artifact rejection (270 remaining trials of 790 trials in the TMS blocks, due to excessive muscular artifacts on temporal electrodes). Overall, behavioral TMS data from 10 participants and EEG data from 9 were analyzed. All participants gave written informed consent before the experiment. Standard exclusion criteria for TMS were applied: pregnancy, metallic implant, cardiac or neurological health condition, and specific medication. The study was approved by the local ethics committee "Sud-Ouest et Outre-Mer I" with protocol number 2009-A01087-50 and followed the Code of Ethics of the World Medical Association (Declaration of Helsinki).

EEG Acquisition and TMS Apparatus

Participants were placed 57 cm from the screen (36.5° × 27° of visual angle), with their head maintained by a chinrest and headrest in front of them and a 70-mm figure-of-eight coil pressed over their occipital cortex. TMS pulses were applied using a Magstim Rapid^2 stimulator (3.5 T) producing a biphasic current (Carmarthenshire, UK). EEG was simultaneously recorded using an ActiveTwo Biosemi system (Amsterdam, The Netherlands) (64 channels). CMS (common mode sense) and DRL (driven right leg) electrodes, both placed on the participant's face to minimize TMS-induced EEG artifacts, were used as reference and ground. Eye movements were monitored with an EOG. Postacquisition, the data were downsampled to 512 Hz, re-referenced to average reference, and epoched from −1500 to +1000 msec relative to stimulus onset. To minimize the impact of TMS-induced pulse artifacts, the EEG data from −1 to +150 msec around each TMS pulse were erased and replaced with a linear interpolation of the window boundaries. Note that we verified that the slope of this linear interpolation was unrelated to perceptual outcome: The comparison across participants of the averaged slopes of correct versus incorrect trials was not significant, $t(8) = 0.95$, $p = .37$. Finally, the data were screened manually for any remaining artifacts (eye movements, muscle contractions, etc.).

Stimulus Procedure

Participants performed 22 blocks of 52 trials: 16 blocks with a double-pulse of TMS applied on each trial (see TMS Procedure) and 6 blocks (randomly interspersed among the other 16) with no TMS. In both types of blocks, participants performed a difficult visual search: report the presence or absence of a target (letter "T") among distractors (letters "L"). On each trial, four letters were presented after a random and uniformly distributed intertrial delay of 1.5–2.5 sec: either four Ls or three Ls and one T (each letter could be presented randomly in four orientations: 0°, 90°, 180° or 270° from upright). The four letters were presented on a virtual ring at constant eccentricity either on the lower right or on the lower left visual field (see TMS Procedure for the TMS blocks). The stimuli disappeared after a given SOA and were replaced by visual masks (a square with a "+" in the middle). SOAs were adjusted individually in a preliminary experiment via a staircase procedure to achieve about 75% correct search performance (the mean ± standard deviation of individual SOAs was 118 ± 52 msec). The total presentation duration (search array + masks) was 500 msec. Participants reported the presence or absence of the target by pressing a button on the keyboard. All participants used the right hand for button press.

EEG Analysis

As the stimulus presentation was lateralized on each trial to the left or right side, we reasoned that correlates of stimulus processing and attentional selection may not be found on a given fixed set of electrodes, but rather on different electrode groups depending on the side of presentation (i.e., electrodes "contralateral" or "ipsilateral" to the search array). Therefore, we permuted the electrode locations for every trial in which the search array had been presented on the right side: We replaced the left-hemisphere electrodes by the right ones and vice versa (midline electrodes were unaffected). With this new electrode assignment, left-hemisphere electrodes always correspond to those ipsilateral to the search array, and right-hemisphere electrodes correspond to contralateral ones. Phase information was computed using a time–frequency decomposition (akin to wavelets) on single trials (Dugue, Marque, & VanRullen, 2011a; VanRullen, Busch, Drewes, & Dubois, 2011), based on a function from the EEGLAB software package (Delorme & Makeig, 2004) under Matlab (The MathWorks, Natick, MA) (function timefreq with the

parameters "cycles" and "freqs" set to [1, 15] and [2, 100], respectively; this produces a decomposition at frequencies increasing logarithmically from 2 to 100 Hz, whereas the length of the filter window changes linearly from 1 to 15 cycles). At any time point (pre- and poststimulus) and frequency, we calculated the phase-locking across trials (norm of the average across trials of the normalized complex vector resulting from the time–frequency decomposition) separately for each experimental condition: correct versus incorrect search trials.

Poststimulus EEG Phase-locking Analysis

Poststimulus EEG was analyzed only for trials in which no TMS pulse was applied to avoid any contamination by pulse artifacts. In the poststimulus period, the presentation of the search array and the ensuing search process are expected to evoke a large event-related response, meaning that most of the trials will tend to display similar phase values. We hypothesized that correct search performance could be characterized by a stronger phase-locking across trials; incorrect search, on the other hand, could be associated with a departure from the optimal search process and, therefore, with more dispersed phase values across trials. Consequently, we computed the phase-locking difference between correct and incorrect trials. We subsampled the number of correct trials to equalize it to the number of incorrect trials. We iterated this trial selection procedure a hundred times for each electrode and each participant and averaged the iterations. We then computed the phase-locking difference for all time–frequency points, averaged over all 64 electrodes. Statistical significance was assessed by comparing the phase-locking difference between correct and incorrect conditions to a surrogate distribution obtained via a permutation procedure, consisting in randomly assigning the trials to one or the other condition (and applying again a subsampling procedure 100 times for each surrogate to equate the number of trials in the two conditions) and recalculating phase-locking difference values to obtain a surrogate phase-locking difference value distribution (characterized by its mean and *SD*) under the null hypothesis that correct and incorrect search trials are derived from the same phase distribution. The experimentally observed phase-locking difference value at each time–frequency point was converted into a *z*-score by comparing it to the mean and *SD* of the corresponding null distribution; finally, the *z*-score was expressed as a *p* value and corrected for multiple comparisons with the false discovery rate (FDR) procedure (FDR = 10^{-4}, corresponding to a *p* value threshold of 3.9×10^{-6}). To ensure that the results were not due to any single participant (outlier), we discarded each participant one by one from the analysis and recomputed FDR-corrected *p* values (FDR = 10^{-4}, corresponding to *p* value thresholds 6.1×10^{-6}). This procedure did not reveal an outstanding role for any of the experimental participants (i.e., no outlier).

Poststimulus Amplitude Activity

Oscillatory amplitude values were computed trial-by-trial (baseline-corrected using the time period [−400 to 0 msec] as baseline) and contrasted between correct and incorrect conditions as a *z*-score (i.e., the difference was expressed in units of standard error across trials). The *z*-scores were then combined across all electrodes and participants.

Prestimulus EEG Phase Opposition Analysis

Prestimulus EEG data were analyzed together for the TMS and no-TMS trials to maximize statistical power (we also verified that our main results held separately for each of these conditions). In the prestimulus period, because of the randomized intertrial interval, we expected a uniform phase distribution of the spontaneous EEG signal over all trials. Consequently, any significant phase-locking occurring in one condition (e.g., correct search trials) would need to be matched by an equivalent phase-locking (toward the opposite phase angle) in the other condition (e.g., incorrect search trials). In other words, no difference in phase-locking was expected in the prestimulus period, but rather a potential phase opposition between correct and incorrect trials. Phase-locking values were computed separately for correct and incorrect search trials and then averaged across the two conditions and across all electrodes. This average was then compared with a surrogate distribution obtained via a permutation procedure, consisting in randomly assigning (10,000 repetitions) the trials to one or the other condition (keeping the number of trials in each condition constant) and recalculating phase-locking values to obtain a surrogate phase-locking distribution (characterized by its mean and *SD*) under the null hypothesis that both correct and incorrect search trials have a uniform phase distribution. The experimentally observed phase-locking at each time–frequency point was converted into a *z*-score by comparing it to the mean and *SD* of the corresponding null distribution; finally, the *z*-score was expressed as a *p* value (*t* test). *p* Values were corrected for multiple comparisons using the FDR method (FDR = 10^{-3}, corresponding to a *p* value threshold of 5.1×10^{-5}). To ensure that the results were not because of any single participant (outlier), we discarded each participant one by one from the analysis and recomputed FDR-corrected *p* values (FDR = 0.05, corresponding to a *p* value threshold < .007). This procedure did not reveal an outstanding role for any of the experimental participants (i.e., no outlier). Finally, the scalp topography of the *z*-score of the phase opposition values revealed a specific ROI involved in the phase opposition effect. For this ROI, we repeated the previous phase opposition analysis (FDR = 10^{-4}, corresponding to a *p* value threshold of 1.9×10^{-7}). We also performed the same analysis with one-cycle wavelets at all frequencies, with comparable results.

Prestimulus Differential ERP Activity

EEG signals were band-pass filtered between 5.6 and 7.6 Hz using the function EEGFILT from the EEGLAB software (finite impulse response filtering using the window method, attenuation at cutoff frequencies at −6 dB [half the passband gain], filter order = 274 samples). ERPs (electrode Cz) for incorrect trials were subtracted from the correct trials ERPs. A t test against zero across observers was then performed at each time point.

Control Experiment

Eleven participants were recruited to participate in an easy search experiment (control task; only one of them had also participated in the main difficult search experiment). Participants performed 500 trials in which they had to report the presence or absence of a + target among L distractors. The randomization conditions were the same as in the main experiment. In this case, as no TMS was applied and consequently no phosphene was perceived, the stimuli were presented either in the left or in the right hemifield (in randomly interleaved trials), on a virtual circle at 8° eccentricity. We computed the pre- and poststimulus EEG phase and amplitude analyses as described above.

TMS Procedure

The TMS experiment involved two types of tasks that were repeated in alternation (see Figure 1). The phosphene mapping task was intended to determine the spatial location corresponding to the magnetically stimulated retinotopic region. The difficult visual search task was then performed with stimuli at the corresponding spatial location (or, on different trials, at a symmetrically opposite location on the screen, used as a control). After every 104 visual search trials, the experiment reverted to the phosphene mapping task, and so on.

Phosphene Mapping

We used the same protocol as in our previous experiment (Dugue, Marque, & VanRullen, 2011b). Participants fixated at the center of a dark screen. A train of seven TMS pulses at 20 Hz and at 70% of maximal output intensity was applied on the scalp over the assumed V1 region (1 cm

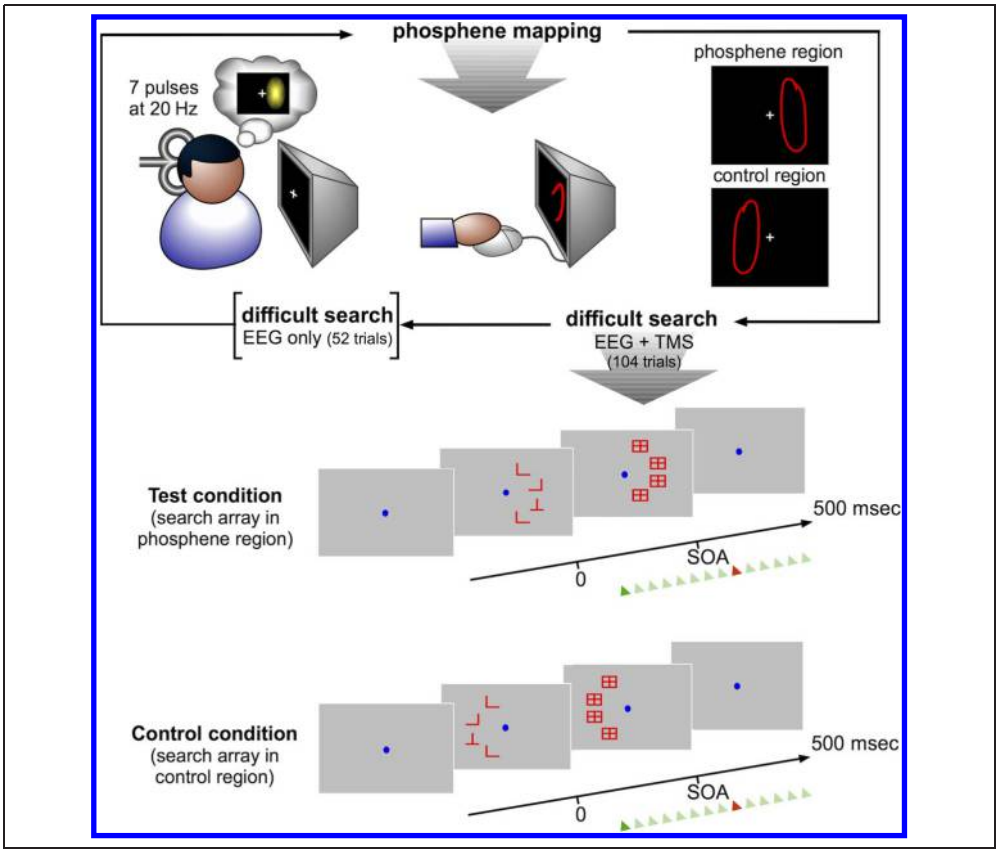

Figure 1. Experimental procedure for TMS blocks. In a first step, participants received seven TMS pulses over occipital cortex (20 pulses per second, 70% output intensity) to induce perception of a phosphene (illusory flash). They indicated the "phosphene region" by drawing it on the screen. The same region was then used in a second step for presentation of the visual search stimuli (so-called test condition). This area corresponds to the aggregate receptive field of the stimulated cortical site, thus ensuring a specific TMS effect. A control condition consisted in displaying visual search stimuli in the symmetric region relative to the vertical midline. The search task required detecting the presence (50% probability) of a target T among L distractors. All four letters were masked by a subsequent pattern, with an SOA that had been individually adjusted to set performance around 75% (without TMS). Two pulses were applied in each trial: one at a fixed delay of 312.5 msec after stimulus onset (red triangle), another one at a randomly determined delay around the first pulse (13 possible delays, represented by green triangles, equally spaced between 112.5 and 437.5 msec). The phosphene mapping procedure was repeated after every 104 search trials (2 blocks of 52 trials) to verify (and potentially update) the position of the TMS coil (and of the corresponding phosphene region). EEG was recorded continuously throughout the experiment. A number of search blocks were also performed without any TMS, intermixed with EEG + TMS blocks.

above the inion). The stimulations were applied either on the left or on the right hemisphere (~2 cm away from the midline) to produce phosphene perception either in the right or in the left hemifield. Immediately after stimulation, participants were asked to draw the outline of the perceived phosphene as precisely as possible using the computer mouse. They were allowed to repeat the stimulation and verify the phosphene outline until they were satisfied with their response. The resulting zone, so-called "phosphene region," was then used during the subsequent visual search trials as the retinotopically specific region of stimulus presentation: "test condition." The symmetrical region in the opposite hemifield was also used as a nonspecific "control region"—we expected that TMS did not affect (or affected to a lesser extent) the processing of stimuli presented in this zone: "control condition." The phosphene mapping procedure was validated only when the spatial extent of the phosphene was deemed sufficient to present the entire search array within this region (i.e., the extent of the phosphene was expected to be at least as large as its eccentricity); otherwise, the TMS coil was displaced by 1 cm and the procedure was repeated, until a suitable phosphene was found.

Difficult Visual Search and dTMS

In half of the trials (pseudorandomly determined), stimuli appeared within the "phosphene region," and within the "control region" in the other half. Half of the TMS blocks had the phosphene region on the left hemifield (i.e., the TMS pulses were applied over the right brain hemisphere) and the other half in the right (TMS pulses over the left brain hemisphere). Double pulses of TMS were applied in each trial at subthreshold intensity (55% of maximal output intensity so that no phosphene perception occurred during stimulus presentation), separated by different intervals. One pulse remained fixed at a latency of 312.5 msec after stimulus onset, based on the main effect found in our previous experiment (Dugue et al., 2011b). The second pulse was applied at 13 other possible delays before or after the first pulse (112.5, 137.5, 162.5, 187.5, 212.5, 237.5, 262.5, 287.5, 337.5, 362.5, 387.5, 412.5, or 437.5 msec after stimulus onset—poststimulus delays under 100 msec were not employed since previous research [Juan & Walsh, 2003] established that TMS interference at such delays is comparable for difficult and easy search tasks and therefore does not reflect attentional effects). The presence of the fixed-latency TMS pulse at 312.5 msec was intended to capitalize on our previous finding (Dugue et al., 2011b) of maximal interference at ~300 msec and thereby allow us to sufficiently disrupt performance on every trial so that a rhythmic influence of the variable-latency TMS pulse (if any) could more easily be measured. This choice was costly: It implies that TMS changes due to the variable-latency pulse cannot be disentangled from those caused by variations in interpulse interval (the delay between the fixed- and variable-latency pulses). On the other hand, this choice was necessary: No significant periodicity of TMS-induced search interference had been obtained in our previous study using only variable-latency pulses (Dugue et al., 2011b). In the end, although it must be acknowledged that the effects of variable pulse latency and interpulse interval cannot be distinguished, this choice of paradigm was legitimate in the sense that any finding of oscillatory TMS modulation (whether caused by one or the other variable) would still support our original prediction of a periodicity in visual search. Search performance data were analyzed in terms of hit rates, because we expected that TMS should specifically affect the target detection.

RESULTS

Ten observers performed a difficult search task, looking for the target letter T among several instances of the distractor letter L. In a preliminary experiment with variable set size (the number of elements on the screen) and response-terminated stimulus presentations, we confirmed that each observer applied an attentional search strategy: search slopes, expressing RT as a function of set size, were significantly positive (36.8 msec per item for target present trials—t test for individual slope against zero: $t(9) = 14.3$, $p < .005$; 64.8 msec per item for target absent trials—$t(9) = 32.1$, $p < .005$). In the main experiment, targets and distractors were unchanged, but set size was fixed to four elements and search arrays were followed by a mask after a SOA (mean SOA ± standard deviation across participants: 118 ± 52 msec) that was individually adjusted to maintain search performance around 75%. EEG was recorded throughout the experiment. In some blocks of trials, a double-pulse of TMS was applied over visual cortex at a critical interval after search array onset; whereas in other blocks, no TMS was applied (this procedure is similar to Romei, Gross, & Thut, 2012, who combined EEG and TMS to investigate cyclic patterns of perception).

Poststimulus EEG Oscillatory Activity Is Higher during Successful Search

If attentional search relies on an iterative selection process, the detection of the search target should involve neuronal signals arising at specific poststimulus moments. A specific poststimulus oscillatory pattern should thus be visible in the participant's EEG when they perform the search task successfully; when search is unsuccessful, on the other hand, the relevant oscillation should be less likely to match this specific pattern. In other words, we predicted that EEG oscillations in a relevant frequency band should be more phase-locked across trials during successful compared with unsuccessful search. To test this prediction, we analyzed oscillatory EEG signals recorded during the search task by means of single-trial time–frequency transforms and computed oscillatory phase-locking across trials at each poststimulus time point and frequency; finally, we contrasted these phase-locking

values for the correct and incorrect search trials. This analysis was performed on trials in which no TMS pulse was applied; therefore, EEG signals were not affected by TMS electromagnetic artifacts and allowed a fully independent test of our predictions.

The difference of phase-locking values between correct and incorrect search trials is illustrated in Figure 2A. This difference was significantly higher than expected by chance (permutation test, FDR-corrected p value threshold = 3.9×10^{-6}). This effect was visible from 100 to 400 msec after stimulus onset and observed specifically in the theta (4–8 Hz) frequency range, with a peak frequency of 6.1 Hz. For that frequency, the temporal profile of the phase-locking difference showed three local maxima at 124, 337, and 554 msec poststimulus. Finally, the corresponding scalp topography revealed that phase-locking differences were maximal over occipital electrodes contralateral to the search array (Figure 2A).

Note that the increase of phase-locking observed for correct trials is compatible with an increase in evoked activity. Indeed, we observed higher induced oscillatory amplitude for correct trials in the theta frequency range (peak at 6.6 Hz) during the poststimulus period (Figure 2B), involving a similar array of occipital, parietal, and frontal electrodes as for the phase-locking effects (Figure 2A). It is notoriously difficult to distinguish oscillatory phase-locking from systematic amplitude increases, and we must thus consider that the phase-locking differences in Figure 2A and amplitude differences in Figure 2B may reflect the same underlying neuronal process (Luck, 2005). However, the difference in timing (with a first peak in phase-locking as early as 124 msec after stimulus onset, while amplitude effects peak at 398 msec) suggests that the two effects could also, in part, involve distinct mechanisms.

Overall, it is clear that not only the phase but also the amplitude of poststimulus theta oscillations play a role in target detection.

Prestimulus Phase Angles Differ for Successful versus Unsuccessful Search

If an appropriate phase-locking of poststimulus theta oscillations is important for search performance, it might also be possible to reveal a signature of this relation at the level of prestimulus, spontaneous oscillations. In this case, we would not expect a difference in phase-locking values between correct and incorrect search, but rather a difference in the average phase angle of the oscillations. Indeed, because spontaneous oscillations preceding an unpredictable stimulus onset event necessarily have a uniform phase distribution across trials, any significant phase-locking toward a particular phase angle for one group of trials (e.g., correct trials) must be matched by an equivalent phase-locking toward the opposite phase angle for the remainder

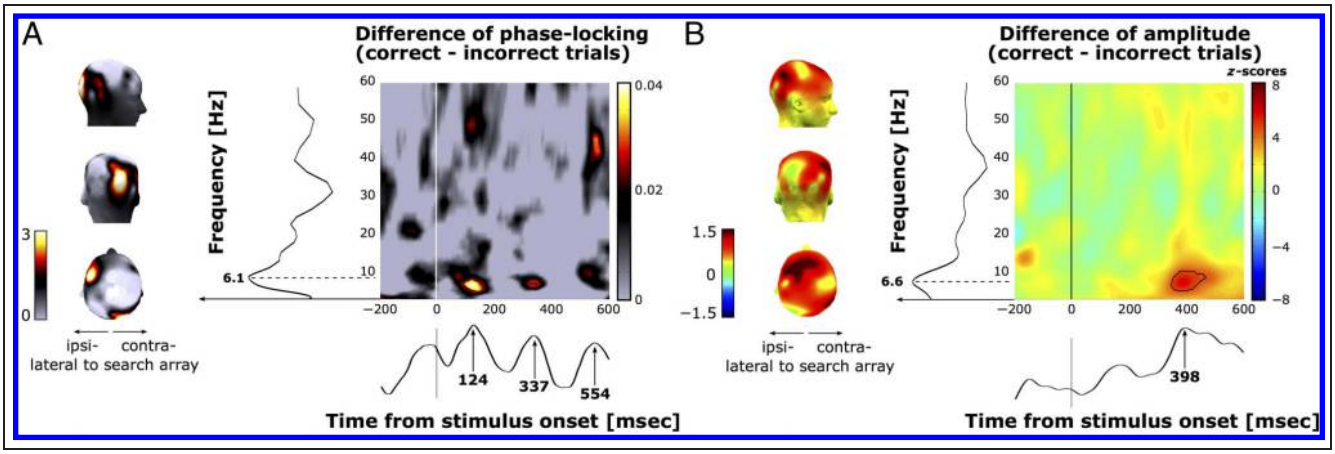

Figure 2. Poststimulus theta EEG oscillatory activity indexes search performance. (A) Time–frequency map of the difference of phase-locking across trials between correct and incorrect search trials over all 64 electrodes. Successful search was characterized by significantly higher phase-locking than expected by chance, in the theta range during the first 400 msec after stimulus onset (black outline denotes significance threshold of a permutation test, FDR-corrected for multiple comparisons; corrected p value threshold = 3.9×10^{-6}). The black curve along the y axis illustrates the frequency profile of the phase-locking difference (averaged difference over interval 0–400 msec) and indicates that the effect peaks within the theta range (maximum frequency = 6.1 Hz). The black curve along the x axis illustrates the temporal profile of the phase-locking difference (averaged difference over frequencies from 5.2 to 7.8 Hz) and reveals three local maxima at 124, 337, and 554 msec after stimulus onset. The corresponding scalp topography (left) of the z-score values computed within the time–frequency window of maximal significance ([24 msec; 224 msec] and [5 Hz; 7 Hz]) shows that the phase-locking difference is maximal over occipital electrodes contralaterally to the search array and also visible on ipsilateral frontal electrodes (possibly reflecting the orientation of a single dipole source located in-between the contralateral occipital and ipsilateral frontal regions). Left- and right-hemisphere electrodes represent ipsi- and contralateral sites, respectively (see Methods). (B) Time–frequency map of the difference in "induced" oscillatory amplitude between correct and incorrect search trials, expressed as a z-score, over all 64 electrodes. Successful search is characterized by significantly higher amplitude in the theta range (maximum frequency = 6.6 Hz), with a maximal effect peaking at 398 msec after stimulus onset (black outline denotes significance after FDR correction for multiple comparisons across time and frequency points; corrected p value threshold = 2.3×10^{-6}). The corresponding scalp topography computed within the time–frequency window of maximal significance ([350 msec; 450 msec] and [4 Hz; 12 Hz]) shows a very similar pattern as for the phase-locking effect.

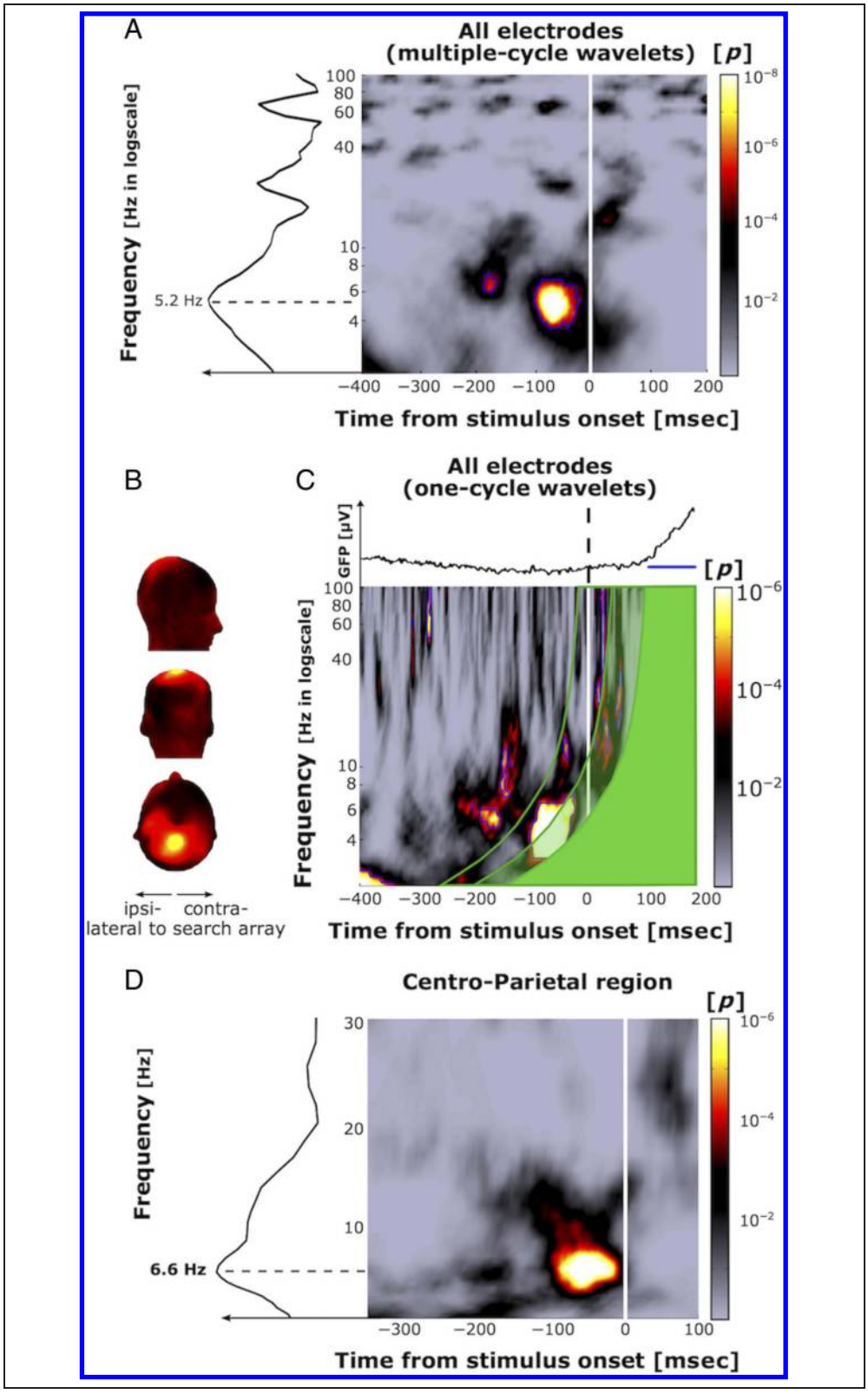

Figure 3. Prestimulus theta EEG phase differs for correct and incorrect search. (A) For each frequency and time point, the phase opposition between correct and incorrect search trials (average over 64 electrodes and 9 participants) was statistically evaluated against surrogate measurements computed over random subsets of search trials. Significant effects indicate that the phase angle of prestimulus EEG oscillations is opposite for correct and incorrect search trials. The color bars (A, C, and D) represent uncorrected p values, whereas the blue outlines (A, C) correspond to significant effects after FDR correction for multiple comparisons across time and frequency points. There is a strongly significant phase opposition (FDR-corrected p value threshold = 6.8×10^{-7}) between correct and incorrect trials in the last 100 msec before stimulus onset, ranging from 4 to 7 Hz. The black curve along the y axis illustrates the frequency profile of the phase opposition (averaged over the last 100 msec prestimulus). Phase opposition peaks in the theta range, at a frequency of 5.2 Hz. (B) The scalp topography of phase-locking values in this time–frequency window ([−100 msec; 0 msec] and [4 Hz; 8 Hz]) shows a centroparietal ROI, centered on the electrode Cz. (C) The prestimulus phase opposition between correct and incorrect search trials was recomputed using one-cycle wavelet analysis. The upper black curve represents the grand-averaged GFP between the 64 electrodes over all participants. The blue dots represent significant difference with the GFP baseline. The plain green area on the time–frequency map indicates the zone of possible influence of evoked activity on the time–frequency signals (based on the wavelet window length at each frequency, centered on the first delay where the GFP significantly differed from baseline, i.e., 111 msec after stimulus onset). The semitransparent and fully transparent green areas illustrate, respectively, the zones of possible influence centered on 50 msec (the earliest reliable visual-evoked activity recorded in humans; Clark & Hillyard, 1996) and 0 msec (stimulus onset). In all cases, some significant prestimulus effects remain outside the zone of possible influence. (D) Phase opposition between correct and incorrect trials (same as in A) recomputed for the centroparietal ROI to estimate its peak frequency. The black curve along the Y axis illustrates the frequency profile of the phase opposition (averaged over the last 100 msec prestimulus). Phase opposition peaks in the theta range, at a frequency of 6.6 Hz.

of the trials (e.g., incorrect trials). This could happen, for example if a specific range of prestimulus phase angles tends to favor the appearance of the appropriate post-stimulus oscillatory pattern (e.g., by minimizing the need for a phase-reset) and consequently to increase the likelihood of a correct search. In such a case, the phase-locking values would not differ between correct and incorrect trials, but the average of these two phase-locking values would be expected to exceed a similar surrogate measure computed over randomly shuffled trial groups (VanRullen et al., 2011). We computed this statistical comparison for all prestimulus time points and all oscillatory frequencies to reveal any significant "phase opposition" between correct and incorrect search trials.

The results (Figure 3A) indicated a significant phase opposition in the last 100 msec before the stimulus onset specifically within the theta (4–8 Hz) frequency range (FDR-corrected p value threshold = 6.8×10^{-7}). The corresponding scalp topography (Figure 3B) highlighted the centroparietal origin of the effect, centered on the electrode Cz. Focusing expressly on this centroparietal ROI, the oscillatory phase opposition appeared to reach a maximum at 6.6 Hz (Figure 3D).

What are the prestimulus phase values that most strongly influence search performance, and how do they differ across participants? To address this question, we computed the difference of ERPs (electrode Cz) between correct and incorrect trials on the EEG signal filtered between 5.6 and 7.6 Hz (Figure 4A). The filtered ERP difference oscillated in the last 300 msec before stimulus onset and periodically diverged from zero (significant t test against zero across participants, $p < .05$). Consequently, this oscillatory behavior had a consistent phase across participants.

This analysis (Figure 4A) and the preceding one (Figure 3) thus reveal that correct and incorrect search performance tend to be associated with different prestimulus phase angles at ~6 Hz. We also explored the reverse relation, that is, how trial-to-trial search performance changes as a function of prestimulus oscillatory phase (computed at the optimal time–frequency point as derived from Figure 3D: 6.6 Hz and −40 msec). To this aim, for each participant and electrode (within the centroparietal ROI), we binned the trials according to their prestimulus phase (9 different phase bins) and calculated search performance for each bin. For each participant, the resulting phase-performance functions were averaged over all centroparietal electrodes and centered with respect to the optimal individual phase bin (the one leading to maximal performance). Finally, these individual phase performance functions were averaged across participants, leaving aside the central phase bin (for which maximal search performance is expected by construction). The resulting grand-averaged function (Figure 4B) indicated that search performance decreased consistently and monotonically by ~7% between the trials at the near-optimal phase and those at the opposite phase (one-way ANOVA: $F(7, 71) = 3.18$, $p < .01$). Altogether, these prestimulus phase effects (Figures 3 and 4) argue in favor of a direct influence of the phase of ongoing theta oscillations on the subsequent search performance.

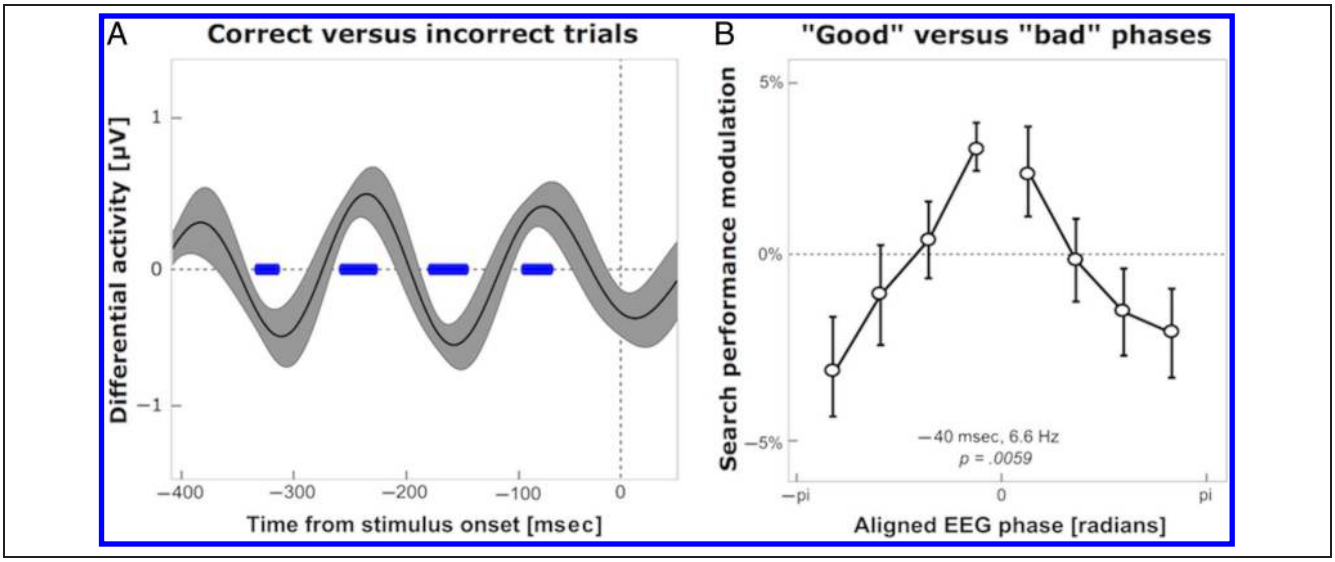

Figure 4. Prestimulus theta EEG phase predicts search performance. (A) ERP difference of the EEG signal filtered between 5.6 and 7.6 Hz between correct and incorrect trials (electrode Cz). Blue dots indicate a significant difference between the differential ERP and zero (t tests against zero across participants; $p < .05$), suggesting that different participants presented comparable oscillatory phases for correct versus incorrect trials. (B) Single trials were sorted in nine nonoverlapping bins according to the EEG phase at 6.6 Hz and −40 msec prestimulus (time–frequency point of maximal significance in Figure 3C). Search performance (deviation from participant-specific average performance) was computed for each bin and averaged over all centroparietal electrodes. For each participant, the bins were then realigned to a maximal performance at zero phase to account for individual differences in optimal phase (the zero-phase bin was then dropped from all subsequent analyses). Search performance decreased monotonically with increasing distance from the optimal phase (one-way ANOVA across the eight nonzero bins, leaving aside the central bin: $F(7, 71) = 3.18$, $p = .0059$). The magnitude of this modulation was ~7%. Error bars represent *SEM*.

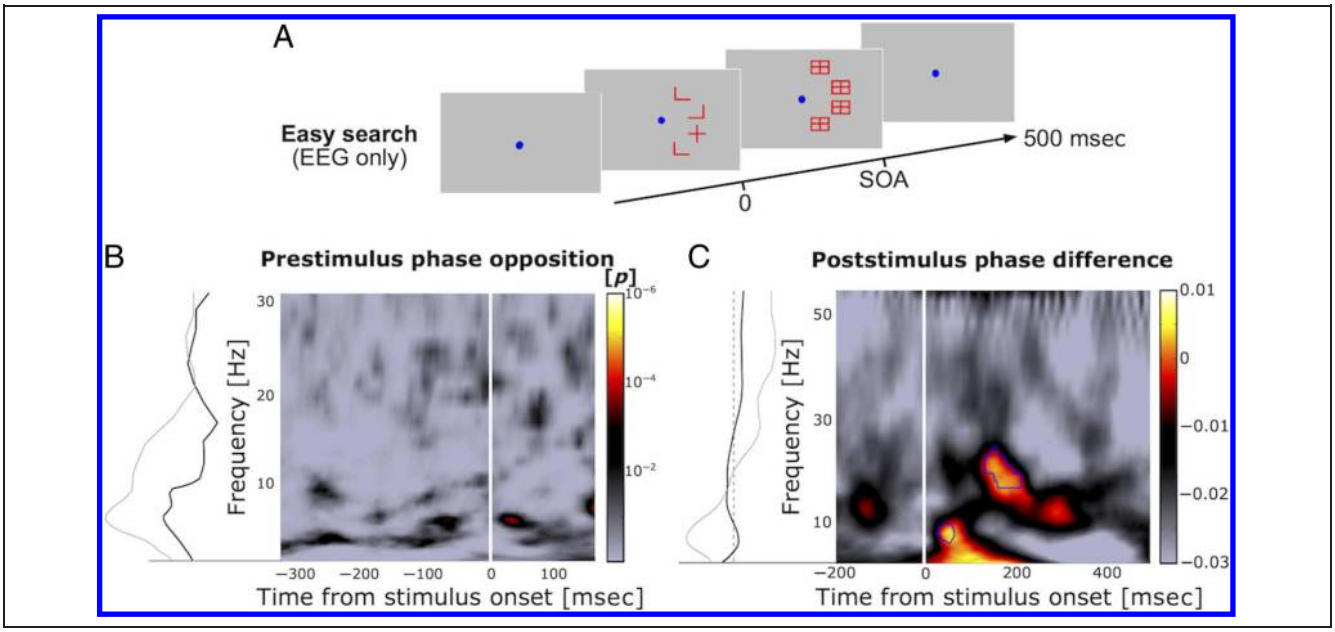

Figure 5. Pre- and poststimulus phase effects for a pop-out search. In a control experiment, we replicated the same phase analyses for an easy ("pop-out") search task. (A) The easy task consisted in finding a "+" sign among randomly rotated letters "L." As in the main experiment, the search array could appear either on the right or on the left, randomly interleaved. (B) Statistical significance of the phase opposition between correct and incorrect trials computed over the previously determined centroparietal ROI (same color scale as in Figure 3C). No significant effect was detected. The black curve along the *y* axis illustrates the frequency profile of the phase opposition (averaged over the last 100 msec prestimulus). For comparison, we report the frequency profile of the phase opposition previously obtained for the difficult search task (gray curve; see Figure 3C). (C) Time–frequency map of the difference of phase-locking across trials between correct and incorrect search trials. Although significant differences between correct and incorrect trials were detected at early latencies and higher frequencies, the theta-frequency phase-locking difference found in Figure 3 of the main manuscript was not replicated here. The black curve along the *y* axis illustrates the frequency profile of the phase-locking difference (averaged difference over interval 0–400 msec). The gray curve corresponds to the frequency profile of the phase-locking difference previously obtained for the difficult search task (see Figure 2A).

EEG Oscillatory Correlates Are Specific to Difficult Search Tasks

In a separate control experiment, we assessed whether similar EEG oscillatory phase effects would also exist for an "easy" search task (see Figure 5 and Methods). Eleven participants searched for a target symbol + among distractor letters L; search was efficient, as indicated by near-zero search slopes (3.1 msec per item for target present trials—t test for individual slope against zero: $t(10) = 1.7$, $p = .02$; 4.2 msec per item for target absent trials—$t(10) = 1.3$, $p = .23$). For this experiment, we computed both prestimulus EEG phase opposition (Figure 5B) and poststimulus EEG phase-locking difference (Figure 5C) as done previously. No significant effect was observed in the theta-frequency band in either case, suggesting that the periodicities observed in the main experiment were specifically associated with the attentional selection process of the difficult search task.

Pre- and Poststimulus Phases Are Linked through a Partial Phase Resetting

The above results indicate that the phase of theta oscillations both before (Figures 3 and 4) and after stimulus onset (Figure 2) can influence the outcome of a difficult search process. Prestimulus, successful search is characterized by an optimal theta oscillatory phase angle, whereas unsuccessful search is associated with the opposite phase angle. Poststimulus, that is, during the search itself, successful trials present more consistent theta phase values (i.e., higher phase-locking or intertrial coherence), whereas unsuccessful trials are associated with more variable theta phase values. Are these two effects related, and if so, by which mechanism? To address this question, we followed over time the phase-locking of a given theta oscillatory signal, recorded at 6.6 Hz on electrode CPz, with the frequency and electrode maximizing the effect shown in Figure 3. Before stimulus onset (−40 msec, corresponding to the peak effect in Figure 3D), theta phase values had a uniform distribution across all trials (Figure 6A; $p = .49$; von Mises kappa coefficient, representing the amount of phase-locking, of 0.03). This is expected, because spontaneous oscillations recorded before an unpredictable stimulus event cannot bear any specific phase relation to this event. Note that this result also confirms that the prestimulus phase effects we report (e.g., Figure 3) are not contaminated by poststimulus phase-locking or evoked activity—a potential concern when using noncausal filtering and wavelet decomposition (see Methods

and Figure 3C). After stimulus onset (+124 msec, corresponding to the peak effect in Figure 2A), the phases of the same theta oscillation presented a significant intertrial coherence (Figure 6B; kappa = 0.25; $p < .0001$). This implies that the stimulus onset had induced a phase reset of the ongoing theta oscillation. If this phase reset was absolute, however, the poststimulus phase would be fully independent of the prestimulus phase value; there would be no memory of prestimulus oscillatory phase during the search process itself; in this case, it would be difficult to explain the influence of prestimulus phase on search performance (Figures 3 and 4). On the contrary, we found that the stimulus-induced phase reset was not absolute but only partial. Figure 6C shows the distribution of trial-by-trial phase differences between post- and prestimulus time points. An absolute phase reset would have produced a uniform distribution, because pre- and poststimulus phase angles would be unrelated (and because the prestimulus phase distribution is itself uniform). Instead, we found a significant intertrial coherence for this difference (Figure 6C; kappa = 0.16, $p < .0001$), implying that pre- and poststimulus phases are linked by a partial phase resetting. This provides a mechanism by which prestimulus phases can eventually influence the outcome of the search process.

It is important to note that we employed the term "phase reset" here in a strictly mathematical sense to describe a situation in which poststimulus phases are more concentrated than prestimulus phases. This kind of reset has been suggested to reflect either the addition of an evoked neuronal response onto brain oscillations or the reinitialization of ongoing oscillations (Sauseng et al., 2007; Makeig et al., 2002; Sayers, Beagley, & Henshall, 1974), but our mathematical usage of the term does not presuppose either of these two interpretations.

In the final analysis, we asked whether the oscillatory pattern observed in the EEG is supported by a periodicity at the behavioral level during the TMS blocks at the same frequency.

TMS over Visual Cortex Interferes Periodically with Attentional Search

EEG results indicate that successful performance in the difficult visual search task that we used is associated with a specific neuronal oscillation in the theta-frequency band. We thus predict that TMS interference in this attentional search would reveal a periodicity of visual information processing at the same frequency.

On every trial of the TMS blocks, two pulses of TMS were applied over early visual cortex while observers performed an attentional or "difficult" search task (L vs. T; see Figure 1). One pulse was systematically applied at 312.5 msec after search array onset ("fixed" pulse). This value was derived from a previous experiment (Dugue et al., 2011b) in which two TMS pulses separated by 25 msec were applied at various latencies: although every latency beyond 100 msec proved innocuous to an "easy" search task (L vs. +; see also Juan & Walsh, 2003), TMS pulse pairs applied at 300–325 msec significantly decreased performance in the "difficult" search task (L vs. T). Therefore, in the present experiment, we sampled TMS latencies around that point (312.5 msec) to investigate the possible existence of a periodic pattern of interference in search performance. Consequently, the second pulse ("variable" pulse) was applied at various delays around the first one (from 112.5 to 437.5 msec after stimulus onset, in steps of 25 msec). The search array was either entirely comprised within the retinotopic location affected by the TMS pulses ("test condition," based on independent retinotopic phosphene mapping sessions, see Figure 1 and Methods), or was presented at the corresponding location in the opposite visual hemifield ("control condition"). This latter condition was used as a baseline, taking into account all nonspecific effects of TMS, that is, those that affect the entire visual field rather than the retinotopic region of the stimulated cortical location.

The effect of TMS on search performance was computed as the difference of hit rate (probability of correct target

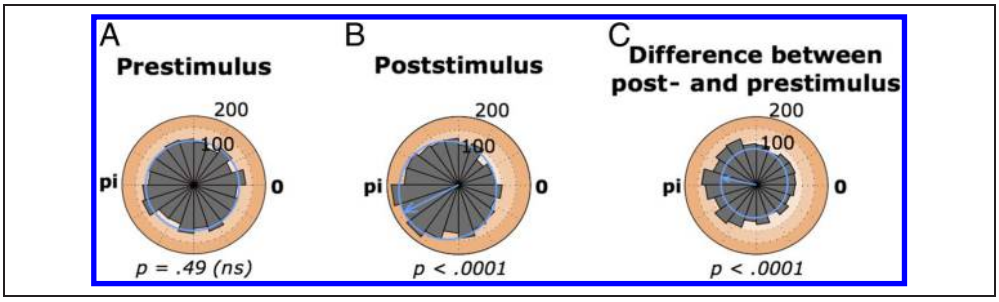

Figure 6. Linking pre and poststimulus activity. Trial-by-trial phase distribution of theta oscillatory activity (6.6 Hz) recorded over electrode CPz, before and after stimulus onset. (A) Prestimulus phase distribution (−40 msec) over all trials. The phase values are uniformly distributed, that is, there is no significant phase preference (von Mises distribution, represented by the blue circle: kappa = 0.03; $p = .49$). (B) Poststimulus phase distribution (+124 msec), over all trials. The phase values are significantly locked to a particular angle, represented by the arrow (von Mises distribution: kappa = 0.25; $p < .0001$). This implies a phase reset induced by the stimulus onset. (C) Distribution of trial-specific differences between post- and prestimulus phases over all trials. This analysis was performed on data obtained from a one-cycle wavelet decomposition to ensure that there was no overlap between the pre- and poststimulus wavelet windows (see Methods). The phase differences are significantly locked to a particular angle (von Mises distribution: kappa = 0.16; $p < .0001$). Because an absolute phase reset would have produced a uniform distribution, this phase-locking implies that the stimulus-induced phase reset was only partial.

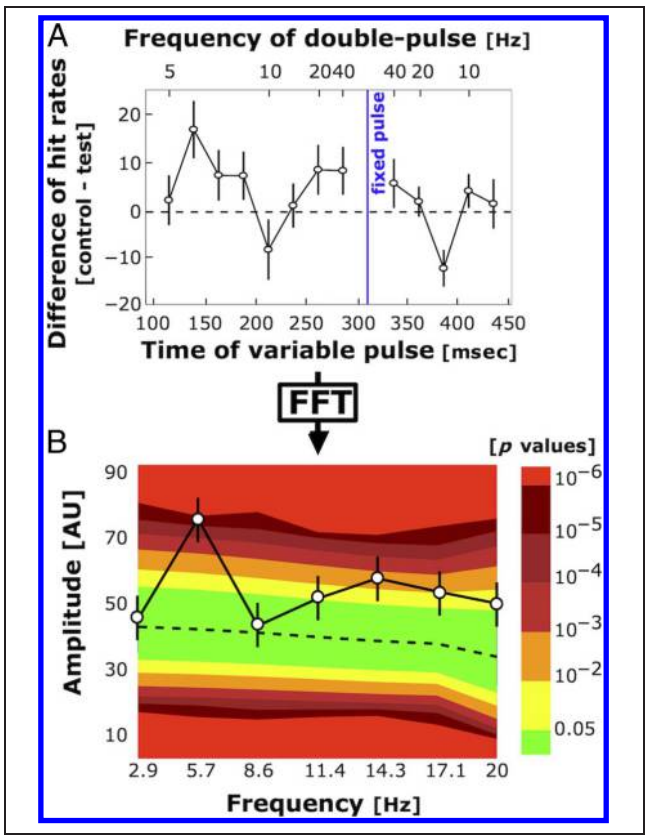

Figure 7. TMS-specific search impairments occur periodically. (A) Difference of hit rates between search trials in which stimuli were displayed in the control condition versus the test condition (10 participants), as a function of the latency of the variable TMS pulse ($t_{variable}$). The time of the fixed pulse was chosen based on a previous TMS experiment employing the same search task at the moment of maximal TMS interference (Dugue et al., 2011b). Positive values represent an impairment of search performance by TMS, whereas negative values correspond to search performance facilitation by TMS. A repeated-measures one-way ANOVA, corrected using the Huyhn–Feldt sphericity correction, showed a significant main effect of TMS latency, $F(12, 129) = 2.3$, $p = .0171$. The hit rate fluctuations as a function of TMS latency suggest a quasiperiodic pattern of TMS interference on visual search performance. On the upper *x*-axis, the difference of hit rates is also represented as a function of the frequency of the TMS double-pulse (inverse of the delay between the variable and fixed pulses). The frequency of maximal interference was 5.7 Hz. (B) Amplitude spectrum of TMS-induced modulations, obtained via a fast Fourier transform of the data in (A). Background colors represent significance of a Monte Carlo statistical test to reject the null hypothesis that TMS latency has no effect on search performance. The significant peak at 5.7 Hz ($p < 10^{-5}$) indicates that the curve in (A) oscillates at this specific frequency. (A, B) Error bars represent *SEM*.

detection) between the control and test conditions. Positive values correspond to an impairment of search performance by TMS, whereas negative values would indicate performance facilitation. When this hit rate difference was plotted as a function of the latency of the "variable" pulse (Figure 7A), two positive and two negative peaks were apparent, which combined to form two cycles of an oscillation with a period of 175 msec, corresponding to a frequency of ~5.7 Hz (a repeated-measures one-way ANOVA, corrected using the Huyhn–Feldt sphericity correction, showed a significant temporal modulation of hit rates: $F(12, 129) = 2.3$, $p = .0171$). It is interesting to note that the two peaks of TMS interference correspond approximately to the first two moments of maximal EEG phase-locking observed in the EEG data set (Figure 2A), although the two data sets are fully independent. Considering not the absolute latency of the "variable" pulse, but rather the interval between this pulse and the "fixed" pulse brought about the same conclusion: The double-pulse of TMS caused maximal interference on search performance when applied at a frequency of 5.7 Hz (repeated-measures one-way ANOVA: $F(7, 79) = 2.7$, $p < .02$). Finally, the pattern of TMS-induced performance modulations represented in Figure 7A was statistically evaluated in the frequency domain (Figure 7B). We applied a fast Fourier transform to compute the amplitude spectrum of TMS-induced performance modulations. The significance of each oscillatory component was assessed by nonparametric statistics. Monte Carlo simulations were performed under the null hypothesis that each participant's hit rates in the test and control conditions were independent of TMS latency (10^6 iterations). For each iteration, we recomputed the grand-averaged curve of the difference of hit rates between test and control condition and then its amplitude spectrum. For each oscillatory frequency, we then sorted these surrogates in ascending order and calculated confidence intervals and the corresponding p values (see Figure 7B). The performance modulation at 5.7 Hz was found to be highly significant ($p < 10^{-5}$). Taken together, the results in Figure 7 indicate that early visual cortex is involved at two specific and well-separated moments in the difficult search task that we used. This confirms our prior EEG results and again suggests a periodicity peaking at a theta frequency.

Because our search stimuli were masked by a subsequent pattern to adjust each participant's performance around 75%, many of the TMS pulses were actually applied while the masks were displayed on the screen, instead of the letters (this was necessary to constrain search performance around 75% correct and to avoid eye movements; even short presentation durations, however, can entail an attentional search strategy; Wolfe, 1998; Bergen & Julesz, 1983). Consequently, one might argue that TMS interfered with the processing of the mask, rather than with the search itself. If this was true, however, then the observed TMS interference pattern should be even stronger when expressed relative to mask onset rather than stimulus onset. On the contrary, we did not observe any significant performance modulation (unbalanced one-way ANOVA: $F(14, 112) = 0.37$; $p = .97$) nor any periodic pattern of interference (Monte Carlo simulations, $p > .05$) after subject-by-subject realignment of TMS latencies to mask onset (data not shown). This confirms that the theta periodicity revealed by our procedure is inherent to visual search rather than to backward-masking processes.

The apparent decrease in TMS interference at 212.5 and 387.5 msec (Figure 7A) was a priori unexpected and requires explanation. Indeed, a decrease in interference implies higher performance for search arrays in the phosphene region compared with the control region. There are thus two possible (and nonexclusive) interpretations: either the TMS pulse at these delays had a beneficial effect on search in the phosphene region, or it had a detrimental effect on search in the control region. The former situation could happen, for example, if the first TMS pulse modulated the phase of the ongoing oscillatory search pattern in such a way that it could escape the negative influence of the next TMS pulse, applied about 100 msec later. The latter could happen if (slow) lateral connections or (faster) callosal fibers carried some of the TMS effect over to the opposite cortical hemifield; in this case, we may argue that the out-of-phase pattern of interference between hemispheres could reflect periodic switching of attention across space, as suggested, for example, by Fiebelkorn, Saalmann, and Kastner (2013), Landau and Fries (2012), or VanRullen, Carlson, and Cavanagh (2007).

To summarize, the TMS blocks revealed a theta periodicity in the pattern of interference created by the variable-latency TMS pulse—although it must be emphasized that, at this point, this conclusion may well be limited to a situation in which a fixed TMS pulse is also applied on every trial at 312.5 msec poststimulus.

DISCUSSION

We used three independent measurements to assess the temporal dynamics of attention during a difficult visual search task (L vs. T). First, successful search performance was associated with different amounts of poststimulus phase-locking and amplitude for theta-frequency EEG oscillations. Second, the phase angle of ongoing EEG theta oscillations just before stimulus onset was found to influence subsequent search performance. Third, TMS-induced interference results demonstrated that early visual cortex was involved periodically during the search process at a theta frequency (4–8 Hz). For all three measurements, the theta-frequency band produced the largest effects. No corresponding EEG oscillatory effect was found during a preattentive (or "easy") search task (see Figure 5). Overall, these results point to theta oscillations as a periodic marker of attentional visual search.

Previous findings already suggested that certain aspects of attention rely on periodic theta-frequency sampling. For example, VanRullen et al. (2007) used a computational model of psychometric functions during a change detection task to determine that attention relies on periodic sampling (~7 Hz). Busch and VanRullen (2010) found that the detection of a threshold visual stimulus is facilitated by attention in a periodic manner that can be indexed by theta-frequency prestimulus EEG oscillations. More recently, Landau and Fries (2012) demonstrated in a psychophysical experiment that attention samples visual stimuli around the same frequency. The present findings, however, advance significantly beyond these past reports by characterizing in a single task the entire functional interplay between spontaneous (prestimulus) oscillatory brain states, poststimulus oscillations, and successful attentional performance. In addition, there has been little experimental evidence so far for a periodic attentional sampling during visual search—although numerous models and theories of visual search have postulated such periodicities (Rodriguez-Sanchez et al., 2007; Hamker, 2004; Deco et al., 2002; Itti & Koch, 2001; Treisman, 1998; Treisman & Souther, 1985; Treisman & Gelade, 1980). A recent electrophysiological study in the FEFs of macaque monkeys (Buschman & Miller, 2007, 2009) revealed a sequential neuronal response to the search items during a color orientation conjunction search task, with a periodicity in the "beta" frequency range (18–25 Hz). Our findings in humans are globally consistent with this observation, although our main TMS and EEG effects are observed primarily over occipital and parietal sites and in a lower frequency range. This difference in frequency could be because of various factors, such as the study of human versus nonhuman primates, the recording of large-scale EEG signals versus local activity of individual neurons or groups of neurons, the amount of task-specific training, or the intrinsic difficulty of the search task. With respect to this point, it is worth noting that our results may be specific to the search task that we used (rotated L vs. T) and that varying task difficulty or experimental conditions could lead to periodic strategies at different oscillatory frequencies (Dugue & VanRullen, 2014). Therefore, future experiments will need to investigate this question, for instance, by parametrically changing the set size (number of distractors in the search array) or the target-defining properties.

Our findings highlight different electrode locations contributing to the theta-periodicity of attention: TMS poststimulus effects were obtained (by experimental design) on contralateral occipital areas (Figure 7); poststimulus oscillatory EEG phase-locking (Figure 2A) and amplitude effects (Figure 2B) also involved contralateral occipital areas as well as parietal regions (on the same, contralateral side) and frontal regions (on the opposite side); finally, the prestimulus EEG phase effects were mainly localized on central parietal electrodes (Figure 3B)—the absence of lateralization in this prestimulus case makes sense, because the search array has yet to be presented and its presentation side was randomized across trials. Although EEG scalp topographies must be interpreted with caution, these findings seem compatible with standard theories postulating that difficult visual search involves iterative selection by attentional areas (or a "saliency map") of the information processed in early visual regions. The occipital region would thus receive periodic attentional enhancement during the search task (visible as TMS interference in Figure 7 and as EEG phase-locking and amplitude modulations

in Figure 2), whereas the prestimulus phase effects over the centroparietal site (Figure 3) and the poststimulus phase-locking and amplitude effects over parietal and frontal sites (Figure 2) could reflect an ongoing periodicity, intrinsic to the attentional areas supporting the saliency map. In TMS trials, depending on its latency, the pulse could then facilitate or disrupt the normal interareal communication between these two hierarchical levels. One interesting possibility in this respect could be that TMS acts via the reset of theta oscillations (though this conclusion would require further substantiation).

Classically, the involvement of attention in visual search tasks is thought to be manifest in positive search slopes: systematic increases of RT as a function of the number of elements in the search array. The sort of task that we used, for example, is typically found to yield search slopes of 30–60 msec per item (for target-present and target-absent trials, respectively; see Methods). Numerous theories of visual search assume that positive search slopes directly reflect a sequential sampling of the search elements by attention: The more elements there are, the more samples need to be taken before finding the target, the longer the RT (Wolfe, 1998; Wolfe et al., 1989; Treisman & Gelade, 1980). The assumed rate of attentional sampling, however, is not directly proportional to the search slope but depends on many factors, such as how many elements are simultaneously processed in each sample, whether the search is exhaustive or not, and whether previously sampled elements are assumed to be discarded or retained as candidate targets along with remaining elements (Horowitz & Wolfe, 1998, 2001). Another class of search theories postulate that attentional selection is distributed in parallel to the entire search array (Eckstein, Thomas, Palmer, & Shimozaki, 2000; McElree & Carrasco, 1999; Eckstein, 1998; Palmer et al., 1993); in this case, the set size dependence of RTs is explained by a decreasing efficiency of attention when more and more items have to be processed simultaneously. Although the former "sequential" models of attentional selection naturally predict an intrinsically periodic strategy such as the one we revealed here (because attentional samples have to be iterated until the target is found), it must be emphasized that the latter "parallel" models are not altogether incompatible with such a periodicity. Indeed, it is possible to envision that attention simultaneously encompasses the entire search array, but that the corresponding attention samples are periodically refreshed by brain oscillations. The present experiments were not designed to disentangle these two alternatives. Future experiments could do so by testing the spatial extent of individual attentional samples—do they process single items, groups of items, or the entire search array? Meanwhile, the present findings have important implications for both "sequential" and "parallel" theories of visual search, as they constrain the temporal dynamics of the search process: attention appears to sample information periodically, and this periodicity, at least for certain difficult search tasks, lies within the theta range.

Acknowledgments

This research was funded by a EURYI Award to R. V. and in part by the European Union's Seventh Framework Program (FET, Neuro-Bio-Inspired Systems: Spatial Cognition) under grant agreement no. 600785. We thank Ayelet Landau and Patrick Cavanagh for useful comments on the manuscript.

Reprint requests should be sent to Laura Dugué, CNRS CERCO UMR 5549, Pavillon Baudot-CHU Purpan, 31052 Toulouse Cedex, France, or via e-mail: laura.dugue@nyu.edu.

REFERENCES

Bergen, J. R., & Julesz, B. (1983). Parallel versus serial processing in rapid pattern discrimination. *Nature, 303,* 696–698.

Busch, N. A., & VanRullen, R. (2010). Spontaneous EEG oscillations reveal periodic sampling of visual attention. *Proceedings of the National Academy of Sciences, U.S.A., 107,* 16048–16053.

Buschman, T. J., & Miller, E. K. (2007). Top–down versus bottom–up control of attention in the prefrontal and posterior parietal cortices. *Science, 315,* 1860–1862.

Buschman, T. J., & Miller, E. K. (2009). Serial, covert shifts of attention during visual search are reflected by the frontal eye fields and correlated with population oscillations. *Neuron, 63,* 386–396.

Clark, V. P., & Hillyard, S. A. (1996). Spatial selective attention affects early extrastriate but not striate components of the visual evoked potential. *Journal of Cognitive Neuroscience, 8,* 387–402.

Deco, G., Pollatos, O., & Zihl, J. (2002). The time course of selective visual attention: Theory and experiments. *Vision Research, 42,* 2925–2945.

Delorme, A., & Makeig, S. (2004). EEGLAB: An open source toolbox for analysis of single-trial EEG dynamics including independent component analysis. *Journal of Neuroscience Methods, 134,* 9–21.

Dugue, L., Marque, P., & VanRullen, R. (2011a). The phase of ongoing oscillations mediates the causal relation between brain excitation and visual perception. *Journal of Neuroscience, 31,* 11889–11893.

Dugue, L., Marque, P., & VanRullen, R. (2011b). Transcranial magnetic stimulation reveals attentional feedback to area V1 during serial visual search. *PloS ONE, 6,* e19712.

Dugue, L., & VanRullen, R. (2014). The dynamics of attentional sampling during visual search revealed by Fourier analysis of periodic noise interference. *Journal of Vision, 14,* 11.

Eckstein, M. P. (1998). The lower visual search efficiency for conjunctions is due to noise and not serial attentional processing. *Psychological Science, 9,* 111–118.

Eckstein, M. P., Thomas, J. P., Palmer, J., & Shimozaki, S. S. (2000). A signal detection model predicts the effects of set size on visual search accuracy for feature, conjunction, triple conjunction, and disjunction displays. *Perception & Psychophysics, 62,* 425–451.

Fiebelkorn, I. C., Saalmann, Y. B., & Kastner, S. (2013). Rhythmic sampling within and between objects despite sustained attention at a cued location. *Current Biology, 23,* 2553–2558.

Hamker, F. H. (2004). A dynamic model of how feature cues guide spatial attention. *Vision Research, 44,* 501–521.

Horowitz, T. S., & Wolfe, J. M. (1998). Visual search has no memory. *Nature, 394,* 575–577.

Horowitz, T. S., & Wolfe, J. M. (2001). Search for multiple targets: Remember the targets, forget the search. *Perception & Psychophysics, 63,* 272–285.

Itti, L., & Koch, C. (2001). Computational modelling of visual attention. *Nature Review Neuroscience, 2,* 194–203.
Juan, C. H., & Walsh, V. (2003). Feedback to V1: A reverse hierarchy in vision. *Experimental Brain Research, 150,* 259–263.
Kammer, T., Puls, K., Erb, M., & Grodd, W. (2005). Transcranial magnetic stimulation in the visual system. II. Characterization of induced phosphenes and scotomas. *Experimental Brain Research, 160,* 129–140.
Landau, A. N., & Fries, P. (2012). Attention samples stimuli rhythmically. *Current Biology, 22,* 1000–1004.
Luck, S. J. (2005). *An introduction to the event-related potential technique*. Cambridge, MA: MIT Press.
Makeig, S., Westerfield, M., Jung, T. P., Enghoff, S., Townsend, J., Courchesne, E., et al. (2002). Dynamic brain sources of visual evoked responses. *Science, 295,* 690–694.
McElree, B., & Carrasco, M. (1999). The temporal dynamics of visual search: Evidence for parallel processing in feature and conjunction searches. *Journal of Experimental Psychology: Human Perception and Performance, 25,* 1517–1539.
Nowak, L. G., Munk, M. H., Girard, P., & Bullier, J. (1995). Visual latencies in areas V1 and V2 of the macaque monkey. *Vision Neuroscience, 12,* 371–384.
Palmer, J., Ames, C. T., & Lindsey, D. T. (1993). Measuring the effect of attention on simple visual search. *Journal of Experimental Psychology: Human Perception and Performance, 19,* 108–130.
Rodriguez-Sanchez, A. J., Simine, E., & Tsotsos, J. K. (2007). Attention and visual search. *International Journal of Neural Systems, 17,* 275–288.
Romei, V., Gross, J., & Thut, G. (2012). Sounds reset rhythms of visual cortex and corresponding human visual perception. *Current Biology, 22,* 807–813.
Romei, V., Brodbeck, V., Michel, C., Amedi, A., Pascual-Leone, A., & Thut, G. (2008). Spontaneous fluctuations in posterior α-band EEG activity reflect variability in excitability of human visual areas. *Cerebral Cortex, 18,* 2010–2018.
Saalmann, Y. B., Pigarev, I. N., & Vidyasagar, T. R. (2007). Neural mechanisms of visual attention: How top–down feedback highlights relevant locations. *Science, 316,* 1612–1615.
Sauseng, P., Klimesch, W., Gruber, W. R., Hanslmayr, S., Freunberger, R., & Doppelmayr, M. (2007). Are event-related potential components generated by phase resetting of brain oscillations? A critical discussion. *Neuroscience, 146,* 1435–1444.
Sayers, B. M. A., Beagley, H. A., & Henshall, W. R. (1974). The mechanism of auditory evoked EEG responses. *Nature, 247,* 481–483.
Thorpe, S. J., & Fabre-Thorpe, M. (2001). Seeking categories in the brain. *Science, 291,* 260–263.
Treisman, A. (1998). Feature binding, attention and object perception. *Philosophical Transactions of the Royal Society London, Series B, Biological Science, 353,* 1295–1306.
Treisman, A., & Gelade, G. (1980). A feature-integration theory of attention. *Cognitive Psychology, 12,* 97–136.
Treisman, A., & Souther, J. (1985). Search asymmetry: A diagnostic for preattentive processing of separable features. *Journal of Experimental Psychology, 114,* 285–310.
VanRullen, R., Busch, N. A., Drewes, J., & Dubois, J. (2011). Ongoing EEG phase as a trial-by-trial predictor of perceptual and attentional variability. *Frontiers in Psychology, 2,* 60.
VanRullen, R., Carlson, T., & Cavanagh, P. (2007). The blinking spotlight of attention. *Proceedings of the National Academy of Sciences, U.S.A., 104,* 19204–19209.
VanRullen, R., & Thorpe, S. J. (2001). The time course of visual processing: From early perception to decision-making. *Journal of Cognitive Neuroscience, 13,* 454–461.
Wolfe, J. M. (1998). Visual search. In H. Pashler (Ed.), *Attention* (pp. 13–73). London: University College London Press.
Wolfe, J. M., Cave, K. R., & Franzel, S. L. (1989). Guided search: An alternative to the feature integration model for visual search. *Journal of Experimental Psychology: Human Perception and Performance, 15,* 419–433.